
PHYSICS
OF NANOSTRUCTURES

Properties of the VT1-0 Titanium Surface Modified by a Pulsed Ion Beam

I. P. Chernov^{a*}, P. A. Beloglazova^a, E. V. Berezneeva^a, I. V. Kireeva^b,
N. S. Pushilina^a, G. E. Remnev^a, and E. N. Stepanova^a

^a National Research Tomsk Polytechnical University, ul. Lenina 30, Tomsk, 634050 Russia

^b Siberian Physicotechnical Institute, National Research Tomsk Polytechnic University, pr. Lenina 30, Tomsk, 634050 Russia
*e-mail: chernov@tpu.ru

Received June 24, 2014; in final form, November 5, 2014

Abstract—The physicomechanical properties of the VT1-0 titanium surface modified by a pulsed carbon ion beam at a pulse duration of 80 ns, an energy of 200 keV, a current density of 120 A/cm², an energy density of 1.92 J/cm², and various numbers of pulses (four regimes) are studied. Irradiation by the beam leads to hardening of a 1.8- μ m-thick surface layer in titanium, a decrease in the hydrogen sorption rate, a decrease in the grain size, and the formation of twins.

DOI: 10.1134/S1063784215070099

INTRODUCTION

Titanium-based alloys are widely used in medicine, shipbuilding, and aerospace and chemical engineering due to their low density, good biocompatibility, and high corrosion resistance. In addition, these alloys are hydride-forming materials: the penetration of hydrogen into the material volume leads to a decrease in the ductility, the fracture toughness, and subsequent fracture. Therefore, the protection of a part made of these alloys against the penetration of hydrogen is a challenging problem. The use of ion beams is one of the promising methods for creating protective coatings, since they increase the wear resistance, the strength, and the corrosion resistance of a part [1–15]. The authors of [11–14] studied the effect of a pulsed electron beam (PEB) and a pulsed ion beam (PIB) of carbon on the properties of a Zr–1% Nb alloy, and the influence of PEB on a titanium alloy was investigated in [15]. The results obtained demonstrate that irradiation leads to the formation of a modified surface layer, which has a high hardness and wear resistance and decreases the penetration of hydrogen into the alloy volume as compared to the initial unirradiated state (i.e., it increases the hydrogen resistance of the alloy).

The purpose of this work is to study the physicomechanical properties of the commercial-purity VT1-0 titanium surface modified by a pulsed beam of charge particles. As the beam, we used a pulsed carbon ion beam to initiate high-rate heating to the melting temperature of the material and to introduce carbon atoms into the near-surface region of the material.

EXPERIMENTAL

We analyzed rectangular 20 × 10 × 1 mm samples of commercial-purity VT1-0 titanium in the as-delivery state without preliminary annealing. The material was modified using a pulsed carbon ion accelerator at a pulse duration of 80 ns, an energy of 200 keV, a current density of 120 A/cm², and an energy density of 1.92 J/cm². The following four regimes, which had different numbers of carbon beam pulses, were studied: regime 1 ($n = 1$), regime 2 ($n = 3$), regime 3 ($n = 4$), and regime 4 ($n = 6$). The structure of titanium was examined with scanning electron microscopy (SEM) and transmission electron microscopy (TEM) on Philips SEM 515 and EM-125K microscopes, respectively. The structure–phase composition was determined by X-ray diffraction (XRD) on a Shimadzu XRD 7000 diffractometer using CuK α radiation. The nanohardness of the modified layer was measured with a NanoHardnessTester (CSEM) nanohardness tester. Samples were saturated by hydrogen on a PCI GasReactionController setup by the Sieverts method at a temperature of 820 K for 1 h.

RESULTS AND DISCUSSION

Figure 1 shows the surface structure of VT1-0 titanium as a function of the number of PIB pulses. The surface relief points to heating, melting, and partial evaporation of the material in the ion-beam-affecting zone. The surface is seen to be heterogeneous and to have a developed relief with pronounced concentric traces of an ion beam and microcraters. In particular, the formation of microcraters is caused by gas release from the near-surface region of the metal.

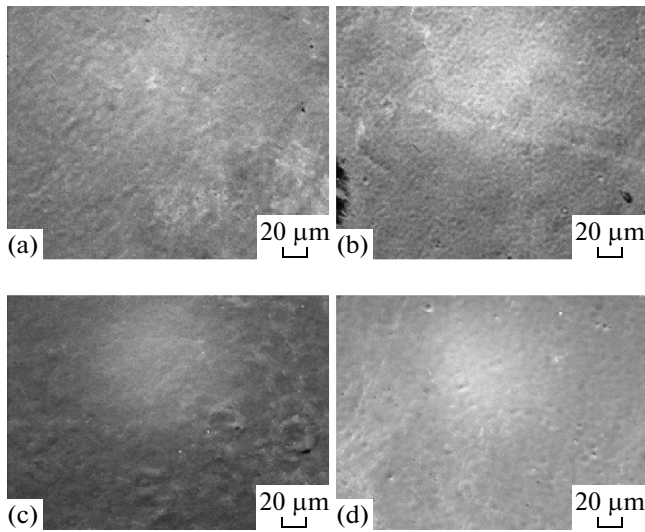


Fig. 1. SEM images of the titanium alloy modified by carbon PIB: (a) initial alloy, (b) after 1 pulse, (c) after 3 pulses, and (d) after 6 pulses.

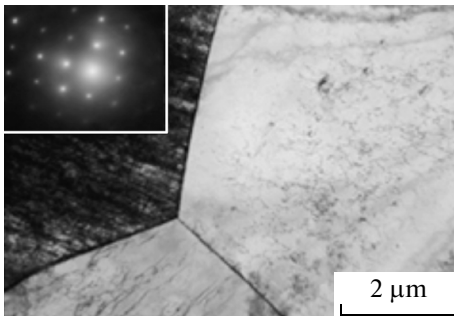


Fig. 2. TEM micrograph of the initial VT1-0 alloy surface.



Fig. 3. TEM micrograph of the VT1-0 alloy surface after the action of 3 pulses.

The structure of the surface layer of VT1-0 titanium before and after irradiation by PIB was analyzed by TEM and XRD. The electron-microscopic investigations of commercial-purity VT1-0 titanium showed that the initial state before the action of carbon PIB consists of equiaxed grains 6–8 μm in size with dislocations inside them (Fig. 2). Irradiation by carbon PIB changes the structure of the surface layer of VT1-0 titanium (Figs. 3, 4). An analysis of bright- and dark-field TEM images showed that the grains acquire a nonequiaxed shape after irradiation by PIB. The nonequiaxed shape can be related to different mobility of grain boundaries after PIB irradiation. The physical cause of the influence of PIB on the grain boundary mobility needs to be investigated. The grain size after PIB irradiation decreases with respect to the initial state, and the decrease in the grain size depends on the PIB irradiation conditions. During PIB irradiation according to regime 2, the grain size decreases insignificantly with respect to the initial state: the grain length is 2.5–3.5 μm and the grain width is 1.5–2 μm (Fig. 3). During PIB irradiation according to regime 4, the grain size decreases substantially with respect to the initial state: the grain length is 1–1.8 μm and the grain width is 0.4–0.8 μm (Figs. 4a, 4b). Electron-microscopic examination (electron diffraction patterns, dark-field images) demonstrates that grains contain twins after PIB irradiation according to regimes 2 and 4. Diffraction analysis shows that twins develop on $(\bar{1}2\bar{1}0)$ planes. During PIB irradiation according to regime 2, the twin length is 2.5–3.5 μm and the twin width is 0.08–0.12 μm (Fig. 3). During PIB irradiation according to regime 4, the twin length is 0.4–0.8 μm and the twin width is 0.04–0.06 μm (Fig. 4).

The decrease in the grain size during PIB irradiation is mainly related to titanium recrystallization after high-rate heating and cooling. During recrystallization, rapid cooling from the melting temperature of VT1-0 titanium causes internal stress fields in new grains, and twins, which occupy almost the entire grain volume after the first carbon beam pulse, are likely to be induced by relaxation of these internal stresses. After the first pulse, a titanium sample represents a composite material consisting of a modified layer 1.8 μm in depth and the retained unmelted initial layer, which can play the role of a substrate and can remember a structure due to the long-range interaction effect. Therefore, as the number of PIB pulses increases (regime 4), the decrease in the grain size can be associated with recrystallization and twinning. The grain size in a titanium alloy was found to decrease upon twinning after low-temperature deformation [16]. The detection of twins in a titanium alloy after carbon PIB irradiation does not contradict the data on twinning in hcp alloys obtained to date. It is known [17] that the sensitivity of hcp alloys to deformation by twinning is explained by a low c/a ratio as compared to

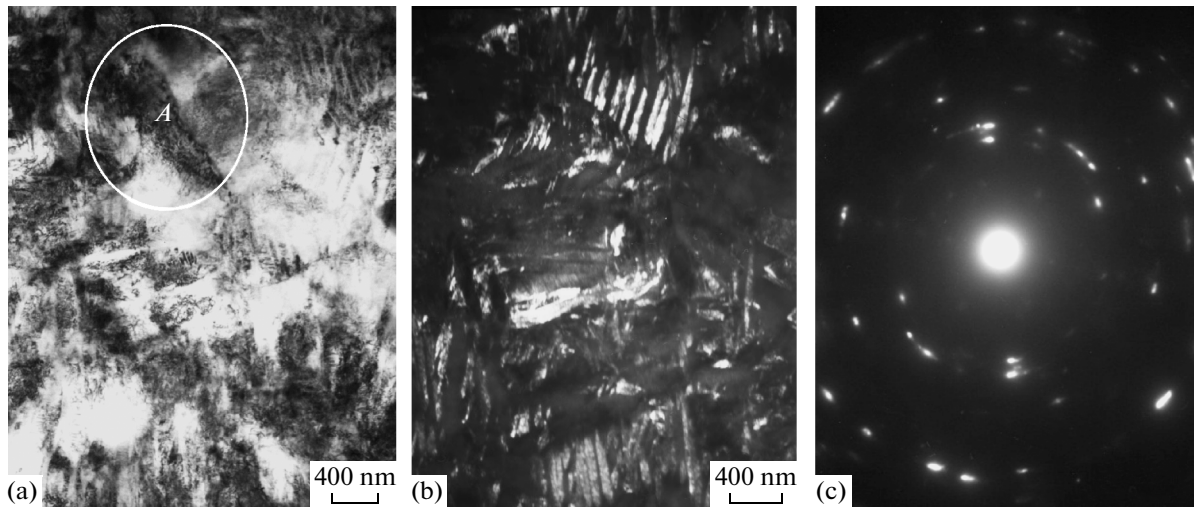


Fig. 4. TEM images of VT1-0 alloy surface after the action of 6 pulses: (a) bright-field image, (b) dark-field image, and (c) electron diffraction pattern from separated region A.

bcc and fcc alloys. XRD data demonstrate that, after PIB irradiation according to regimes 2 and 4, the c/a ratio ($c/a = 1.587$) insignificantly exceeds this ratio ($c/a = 1.585$) in titanium before PIB irradiation (Table 1).

Table 1 presents the phase composition of commercial-purity VT1-0 titanium, which was determined by XRD, after PIB irradiation under various conditions. The X-ray diffraction pattern of VT1-0 titanium in the initial state consists of lines of hcp α -Ti over the entire angular range (Table 1). The introduction of carbon atoms leads to distortion of the titanium lattice. After one pulse (regime 1), carbon atoms do not manifest themselves. An increase in the number of pulses (regimes 3, 4) results in the formation of a carbon phase with a cubic lattice.

To study the mechanical properties of the modified surface layers of commercial-purity VT1-0 titanium, we applied nanoindentation at a load of 5–300 mN. Figure 5 shows the nanohardness of titanium versus the indenter penetration depth. Surface modification is seen to increase the hardness of titanium, and the thickness of the hardened layer is $\sim 2 \mu\text{m}$. The hardening of titanium by PIB is mainly caused by the structure–phase changes in the surface layer of the material due to high-rate heating to the melting temperature and subsequent cooling during irradiation by a pulsed beam. The formation of twins and introduced carbon atoms during PIB irradiation also contribute to the increase in the nanohardness of commercial-purity VT1-0 titanium.

To estimate the hydrogen resistance of the initial and PIB-modified samples, we studied the hydrogen sorption rate during saturation from a gas phase. Figure 6 shows the kinetic curves of the pressure in a measuring chamber during hydrogen sorption by the initial and PIB-modified samples. A decrease in the pressure in the

measuring chamber points to hydrogen absorption by a material. The slope of the kinetic curve characterizes the hydrogenation intensity. Our results demonstrate that the hydrogen sorption rate is $\sim 0.1 \text{ cm}^3 \text{ H}_2/(\text{s cm}^2)$ in initial titanium, $0.03 \text{ cm}^3 \text{ H}_2/(\text{s cm}^2)$ after three PIB pulses, and $0.02 \text{ cm}^3 \text{ H}_2/(\text{s cm}^2)$ after six PIB pulses. Thus, the modified layer decreases the rate of hydrogen absorption by VT1-0 titanium.

To analyze the processes that occur during PIB irradiation, we performed a numerical simulation of the surface irradiation. The determination of the thermal action of PIB on the material is reduced to the solution of a one-dimensional nonstationary heat conduction equation with an internal heat source [18]. The results of calculation of the temperature fields during irradiation by carbon PIB at a pulse duration of 80 ns, an energy of 200 keV, a current density of

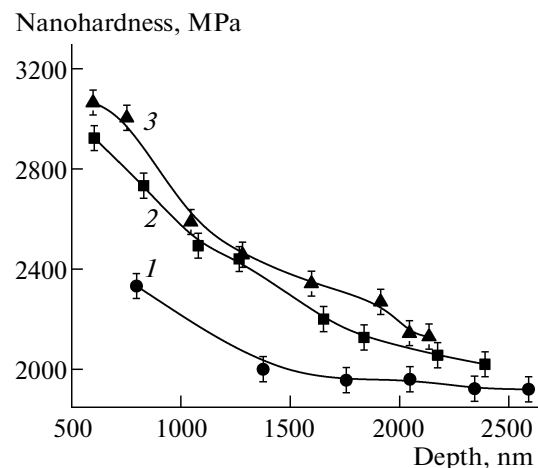


Fig. 5. Nanohardness of the titanium alloy vs. depth before and after irradiation by carbon PIB.

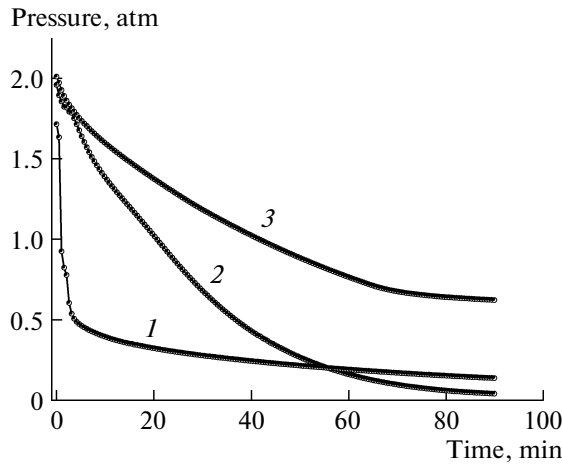


Fig. 6. Kinetic curves of the pressure in a measuring chamber during the sorption of hydrogen by the samples modified by carbon PIB: (1) initial material, (2) after 1 pulse, and (3) after 6 pulses.

120 A/cm², and an energy density of 1.92 J/cm² are presented in Fig. 7 and Table 2. According to the calculations, the temperature at the titanium surface by the end of a pulse (4297 K) exceeds the melting temperature of titanium ($T_{\text{melt}} = 1941$ K), the phase-transition temperature ($T_{\text{phch}} = 1173$ K), and the recrystallization temperature ($T_{\text{rec}} = 1023$ K). The melted layer depth is $r_{\text{se}} = 1.249$ μm .

As is seen from the simulation results (Table 2, Fig. 7), the titanium target has no time to cool down in 2.5 μs from the beginning of irradiation (pulse duration is 80 ns). At this stage, the surface layer temperature is

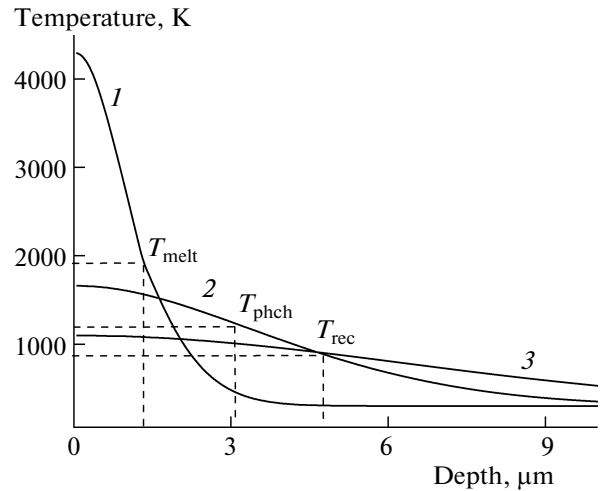


Fig. 7. Depth profiles of the heating temperature in a VT1-0 titanium alloy during carbon PIB irradiation at various times: (1–3) 0.125, 1, and 2.5 μs after the beginning of irradiation. T_{melt} is the melting temperature (~ 1941 K), T_{phch} is the phase-transition temperature (~ 1173 K), and T_{rec} is the recrystallization temperature (~ 1023 K).

1097 K, and no structure–phase changes take place in titanium at this temperature. At a time of 2.5 μs , the modified layer thickness is 1.573×10^{-6} m. Apart from the calculation of thermal fields, we also estimated the kinetics of substance evaporation from the titanium surface. The evaporation layer thicknesses (r_{use}) account for several hundredths of a nanometer, which is negligibly small as compared to the melting depth (Table 2).

Table 1. Phase composition of VT1-0 titanium after PIB irradiation

Sample	Phase	Phase content, vol %	Lattice parameter, Å
VT1-0, initial	Ti	100	$a = 2.9489, c = 4.6747$
VT1-0, PIB, regime 1	Ti	100	$a = 2.9470, c = 4.6868$
VT1-0, PIB, regime 3	Ti	97	$a = 9426, c = 4.6709$
	C	3	$a = 4.6040$
VT1-0, regime 4	Ti	97	$a = 2.9406, c = 4.6670$
	C	3	$a = 4.6021$

Table 2. Depth profiles of the hot rolling temperature in the target at various times

t	T_{surf} , K	r_{use} , m	r_{se} , m
80 ns	4297	1.220×10^{-8}	1.249×10^{-6}
1 μs	1660	1.291×10^{-8}	1.490×10^{-6}
2.5 μs	1097	1.293×10^{-8}	1.573×10^{-6}

CONCLUSIONS

It was experimentally found that irradiation by a pulsed carbon ion beam at a pulse duration of 80 ns, an energy of 200 keV, a current density of 120 A/cm², and an energy density of 1.92 J/cm² hardens the surface layer of commercial-purity titanium to a depth of ~ 2 μm , decreases the grain size, causes the formation of twins in a structure, and decreases the rate of hydrogen absorption by VT1-0 titanium.

The numerical calculations performed to determine the depth profile of the heating temperature at various PIB irradiation times demonstrate that the surface modification during PIB irradiation at the parameters given above is caused by the formation of a liquid phase and its subsequent rapid solidification and recrystallization. The physicomechanical properties of the modified layer studied in this work support this conclusion.

REFERENCES

1. G. E. Remnev, Izv. Tomsk. Politekh. Univ. **303** (2), 59 (2000).

2. M. F. Vorogushin, V. A. Glukhikh, G. Sh. Manukyan, D. A. Karpov, M. P. Svin'in, V. I. Engel'ko, and B. P. Yatsenko, *Vopr. At. Nauki Tekh., Ser.: Fiz. Rad. Povrezhd. Rad. Materialoved.*, No. 3, 101 (2002).
3. Yu. F. Ivanov, I. B. Tsellermaer, V. P. Rotshtein, and V. E. Gromov, *Fiz. Mezomekh.* **9** (5), 107 (2006).
4. Yu. F. Ivanov, Yu. A. Kolubaeva, S. V. Konovalov, N. N. Koval', and V. E. Gromov, *Metalloved. Term. Obrab. Met.*, No. 12, 10 (2008).
5. N. N. Koval' and Yu. F. Ivanov, *Izv. Vyssh. Uchebn. Zaved., Fiz.*, No. 5, 60 (2008).
6. V. P. Rotshtein, Yu. F. Ivanov, A. B. Markov, D. I. Proskurovsky, K. V. Karlik, K. V. Oskomov, B. V. Uglov, A. K. Kuleshov, M. V. Novitskaya, S. N. Dub, Y. Pauleau, and I. A. Shulepov, *Surf. Coat. Technol.*, No. 22, 6378 (2006).
7. B. Gao, S. Hao, J. Zou, W. Wu, and C. Dong, *Surf. Coat. Technol.* **201**, 6297 (2007).
8. T. Grosdidier, J. X. Zou, N. Stein, C. Boulanger, S. Z. Haoc, and C. Dong, *Scr. Mater.* **58**, 1058 (2008).
9. G. A. Bleikher, V. P. Krivobokov, and O. M. Stepanova, *Izv. Vyssh. Uchebn. Zaved., Fiz.* **52** (5), 31 (2007).
10. O. M. Stepanova and V. P. Krivobokov, *Izv. Vyssh. Uchebn. Zaved., Fiz.* **52** (11/2), 186 (2009).
11. I. P. Chernov, S. V. Ivanova Kh. M. Krening, N. N. Koval', V. V. Larionov, A. M. Lider, N. S. Pushilina, E. N. Stepanova, O. M. Stepanova, and Yu. P. Cherdantsev, *Tech. Phys.* **57**, 392 (2012).
12. N. S. Pushilina and I. P. Chernov, *Izv. Vyssh. Uchebn. Zaved., Fiz.* **54** (11/2), 176 (2011).
13. I. P. Chernov, E. V. Chernova, N. S. Pushilina, D. V. Berezneev, A. M. Lider, and K. V. Kryoning, *Appl. Mech. Mater.* **302**, 82 (2013).
14. I. P. Chernov, E. V. Berezneeva, P. A. Beloglazova, S. V. Ivanova, I. V. Kireeva, G. E. Remnev, N. S. Pushilina, A. M. Lider, and Yu. P. Cherdantsev, *Tech. Phys.* **59**, 535 (2014).
15. A. V. Panin, M. S. Kazachenok, O. M. Kretovaet, et al., *Appl. Surf. Sci.* **284**, 750 (2013).
16. V. A. Moskalenko, V. I. Betekhtin, B. K. Kardashev, A. G. Kadomtsev, A. R. Smirnov, R. V. Smolyanets, and M. V. Narykova, *Phys. Solid State* **56**, 1590 (2014).
17. A. Kelly and G. W. Groves, *Crystallography and Crystal Defects* (Longmans, London, 1970).
18. G. A. Bleikher, V. P. Krivobokov, and O. V. Pashchenko, *Heat and Mass Transfer in Solid under Action of High-Power Charged Particle Beams* (Nauka, Moscow, 1999), p. 176.

Translated by K. Shakhlevich